

# 3D kinematics of the equine metacarpophalangeal joint at walk and trot

H. M. Clayton<sup>1</sup>, D. Sha<sup>1</sup>, J. Stick<sup>1</sup>, N. Elvin<sup>2</sup>

<sup>1</sup>Mary Anne McPhail Equine Performance Center, Department of Large Animal Clinical Sciences, College of Veterinary Medicine, and <sup>2</sup>College of Engineering, Michigan State University, East Lansing, Michigan, USA

## Summary

The metacarpophalangeal (MCP) joint and its supporting soft tissues are common sites of injury in athletic horses. Equine gait analysis has focused on 2D analysis in the sagittal plane and little information is available which describes 3D motions of the MCP joint and their possible role in the development of injuries. The aim was to characterize the 3D rotations of the equine MCP joint during walking and trotting. Three-dimensional trajectories of marker triads fixed rigidly to the third metacarpus and proximal phalanx of the right forelimb of healthy horses were recorded at walk ( $n=4$ ) and trot ( $n=6$ ) at 120 Hz using eight infra-red cameras. Kinematics of the MCP joint were calculated in terms of helical angles between the two segments using singular-value decomposition and spatial attitude methods. The ranges of motion were: flexion/extension:  $62 \pm 7^\circ$  at walk,  $77 \pm 5^\circ$  at trot; adduction/abduction:  $13 \pm 7^\circ$  at walk,  $18 \pm 7^\circ$  at trot; and axial rotation:  $6 \pm 3^\circ$  at walk,  $9 \pm 5^\circ$  at trot. Flexion/extension had a consistent pattern and amplitude in all horses and appeared to be coupled with adduction/abduction, such that stance phase extension was accompanied by abduction and swing phase flexion was accompanied by adduction. Axial rotation was small in amount and the direction varied between horses but was consistent within an individual for the two gaits.

## Keywords

Kinematics, joint angles, horse, locomotion, fetlock joint

*Vet Comp Orthop Traumatol* 2007; 20: 86–91

doi:10.1160/VCOT-07-01-0011

## Introduction

The equine metacarpophalangeal (MCP) joint is a high motion joint that plays an important role in locomotor mechanics. To date, the majority of kinematic studies of the MCP joint have been based on sagittal plane 2D data (1–3) or multi-planar analysis in which the analytic planes were referenced to the global coordinate system (4). Misalignments between the plane of motion of the limb segments and the laboratory-based planes are a significant source of error in this type of analysis, especially for small amplitude rotations that have a large signal to noise ratio (5). Therefore, in order to measure adduction/abduction and axial rotations accurately, it is necessary to perform a 3D analysis in which the joint motions are described relative to an anatomically meaningful coordinate system that is aligned with the bone segments. In horses, 3D kinematics have been described during trotting for the tarsal (6) and carpal (7) joints. At the walk and trot, 3D kinematics of the stance phase have been described for the digital joints of the forelimb (8), and the effects of a heel wedge on forelimb kinematics during the stance phase of trot on a treadmill have been measured (9). Three-dimensional kinematics can be applied in 3D inverse dynamic analysis, which provides a deeper understanding of joint function by calculating the torque (moment) across the joint and the mechanical work done by the soft tissues. Previous studies have calculated sagittal plane net joint moments at the MCP joint in sound horses at walk and trot (10–13) and the effects of lameness have been evaluated (14).

The MCP joint and its supporting structures are frequently injured in athletic

horses, especially those that perform at high speed. In racing horses, for example, the MCP joint in the forelimb has a higher incidence of traumatic and degenerative lesions than any other joint (15). As locomotor speed increases, there is an increase in maximal MCP extension (16) and changes in articular contact areas (17). Kinematics of the loaded joint have been implicated in the development of MCP lesions and lameness (17) but the role of movements occurring outside of the sagittal plane in the pathogenesis of injuries has not been explored.

It is anticipated that motion in the axial and transverse planes will be considerably smaller than motion in the sagittal plane and will be affected by errors due to skin displacement over the underlying bones (18). This problem has been overcome using markers that are rigidly fixed to the bones in human subjects (18, 19) and in horses (6–8, 20).

The aim of this study was to use markers rigidly attached to the third metacarpal bone (Mc3) and proximal phalanx (P1) to characterize 3D motions of the equine MCP joint in an anatomically relevant coordinate system for horses walking and trotting in a straight line on a level surface.

## Methods

### Subjects

With approval of the Institutional Committee on Animal Use and Care, six sound horses were used in this study. The physical data for the subjects were: mass:  $433 \pm 63$  kg; height:  $1.47 \pm 0.06$  m.

## Bone-fixed markers

A detailed description of the procedure for rigid attachment of pins to the bones has previously been provided (6). In summary, 4.75 mm diameter Steinmann pins were inserted percutaneously under general anaesthesia into Mc3 and P1 of the right forelimb (Fig. 1).

## Post-operative care

Analgaesics were administered post-surgically: 2 g phenylbutazone<sup>a</sup> was injected intravenously before recovery from anaesthesia, and then phenylbutazone paste<sup>b</sup> was administered orally at a dosage of 2 g b.i.d. for two days followed by 1 g b.i.d. for a further two days. Just prior to data collection, 2% mepivacaine hydrochloride solution<sup>c</sup> was infiltrated locally around the site of pin insertion. All subjects moved willingly and freely at walk and trot during data collection the day after surgery. When data collection was complete, the pins were removed under local anaesthesia.

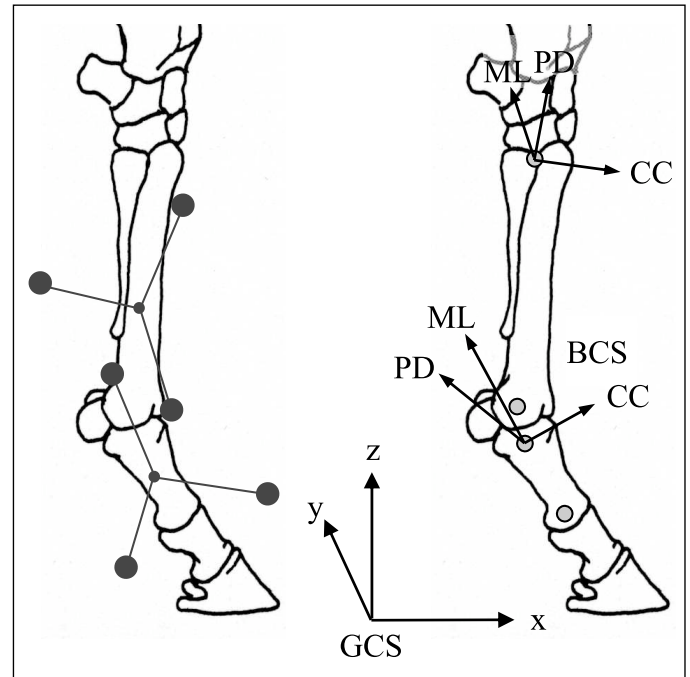
## Bone coordinate systems

A frame with three, 10 mm diameter, reflective, spherical markers was rigidly attached to each pin immediately prior to data collection. The bone-based coordinate systems (BCS) were established by placing the subjects in a normal standing position with the marker triads in place, together with reflective markers attached to the skin overlying the Mc3 and P1 (Fig. 1) in order to establish the anatomically-based bone coordinate systems (BCS). The attachment sites for the skin markers were identified by palpation and radiology. The skin markers were removed before collecting data at the trot.

Skin markers for the metacarpal segment were placed over the dorsal edge of the head

**Fig. 1**

Configuration of markers used in kinematic calculations. Left: Bone-fixed marker triads (dark circles) were used to track the movements of the metacarpal and proximal phalangeal segments and to calculate metacarpophalangeal joint kinematics. Right: Temporary skin markers were placed proximally and distally on the metacarpal and proximal phalangeal segments (light grey circles) to determine bone-based local coordinate systems in the craniocaudal (CC), mediolateral (ML) and proximodistal (PD) directions.



of the second (Mc<sub>med</sub>) and fourth (Mc<sub>lat</sub>) metacarpal bones and distally over the lateral condyle at the attachment of the lateral collateral ligament (Mc<sub>dist</sub>). For the metacarpal BCS, a right-handed coordinate system was developed by first defining the flexion/extension axis as running from Mc<sub>lat</sub> to Mc<sub>med</sub>. The adduction/abduction axis of the metacarpus was defined as running craniocaudally, perpendicular to the plane formed by the flexion/extension axis and the vector running from Mc<sub>lat</sub> to Mc<sub>dist</sub>. Finally, the internal/external rotation axis of the metacarpus was defined as running proximally along the long axis of the bone, perpendicular to the plane formed by the flexion/extension and adduction/abduction axes.

The skin markers on P1 were attached proximally over the tuberosities on the medial and lateral sides of the bone, and distally over the site of attachment of the lateral collateral ligament of the proximal interphalangeal (PIP) joint. The BCS of P1 was established in the same manner as that of Mc3, with the origin of its BCS being located within the bone midway between the two proximal markers.

## Data collection and preprocessing

Data were collected as the horses trotted in hand along a 40 m rubberized runway. In addition, data were collected from four of the six horses at the walk. Three-dimensional kinematic data were collected in the laboratory global coordinate system (GCS) using an eight camera infra-red analysis system with RealTime3.2 software<sup>d</sup> recording at 120 Hz. A volume measuring 5 m by 2 m by 3 m was calibrated using a wand technique. The mean error in measuring a known length within this volume was 0.88 mm.

Each successful trial consisted of a single stride of the right forelimb, starting with stance. Data collected from a force platform<sup>e</sup> embedded in the runway were used to detect the onset and termination of right forelimb stance. Kinematic data were filtered using a fourth-order Butterworth filter with a cutoff frequency of 12 Hz and analyzed using custom-written code in Matlab (MathWorks Inc, Natick, MA, USA). The length of the data was normalized as 101 points for a full stride. Three trials from each

<sup>a</sup> Phenylbutazone, Schering-Plough, Kenilworth, NJ, USA.

<sup>b</sup> Phenylbutazone paste, Schering-Plough, Kenilworth, NJ, USA.

<sup>c</sup> Carbocaine-V, Pharmacia and Upjohn Company, Kalamazoo, MI, USA.

<sup>d</sup> Motion Analysis Corporation, Santa Rosa, CA, USA.

<sup>e</sup> LG-6-4-8000, AMTI, Watertown, MA, USA.

horse were selected for analysis in which forward velocities were closely matched within an individual and with mean values for individual horses in the range 1.45 to 1.54 m/s for walk and 2.8 to 3.2 m/s for trot.

## Calculation of joint kinematics

To calculate the kinematics of joints in the sense of anatomic position (21), the locations of the bone-fixed markers in the GCS were transformed to the corresponding BCS previously defined. Then, the orientation matrices and displacement vectors for the markers while standing and during each frame of walking and trotting were calculated using a singular value decomposition method (22). Lastly, the relative angular

motions (helical angle changes) between the bone segments were calculated using a spatial attitude method (23, 24).

## Data analysis

The data were offset normalized to the limb position at ground contact (25) to reduce variability in the data due to the effect of conformational variations between individuals. Data for three trials of each horse were used to construct a mean curve for that horse. The mean curves for the different horses were then used to develop a group mean curve. The mean  $\pm$  SD for the range of motion of the joint in flexion/extension, adduction/abduction and axial rotation were calculated during the stance phase, the swing phase and the en-

tire stride. The small number of horses did not give sufficient power for statistical comparison between gaits.

Preliminary analysis of the results showed an apparent coupling between flexion/extension and abduction/adduction. It was recognized that this finding might be due to kinematic crosstalk as a consequence of misalignment in establishing the segmental axes of rotation causing some of the flexion/extension motion to be expressed as abduction/adduction (5). To further investigate this possibility, the segmental coordinate system of P1 was rotated  $\pm 10^\circ$  about its longitudinal axis and the adduction/abduction values were recalculated.

## Results

The walk had a velocity of  $1.49 \pm 0.04$  m/s. The stride duration was  $1,242 \pm 97$  ms, with stance occupying  $62.9 \pm 0.7\%$  of stride. During trotting, the velocity was  $3.05 \pm 0.21$  m/s, stride duration was  $754 \pm 29$  ms and stance duration was  $44.3 \pm 1.17\%$  of stride.

Fig. 2 shows the mean angle-time curves  $\pm$  one standard deviation for the three rotations at walk and trot with data normalized to the impact angle. The angular excursions during stance, swing and the entire stride (Table 1) indicate that although flexion/extension was the predominant rotation, there was also a significant amount of adduction/abduction. There was a tendency for all types of movement to be greater at trot than at walk in both stance and swing. The flexion/extension graph (Fig. 2) has a consistent pattern between horses. In walk, the stance phase extension was prolonged with a tendency toward two peaks separated by a slight reduction of extension. In trot there was a single cycle of extension. Both gaits had two distinct flexion peaks in the swing phase.

All horses showed abduction during stance and a double-peaked cycle of adduction during swing with the adduction/abduction peaks being temporally related to the flexion/extension peaks in both walk and trot (Fig. 2). Adduction/abduction was linearly related with flexion/extension (correlation coefficient 0.995). When the seg-

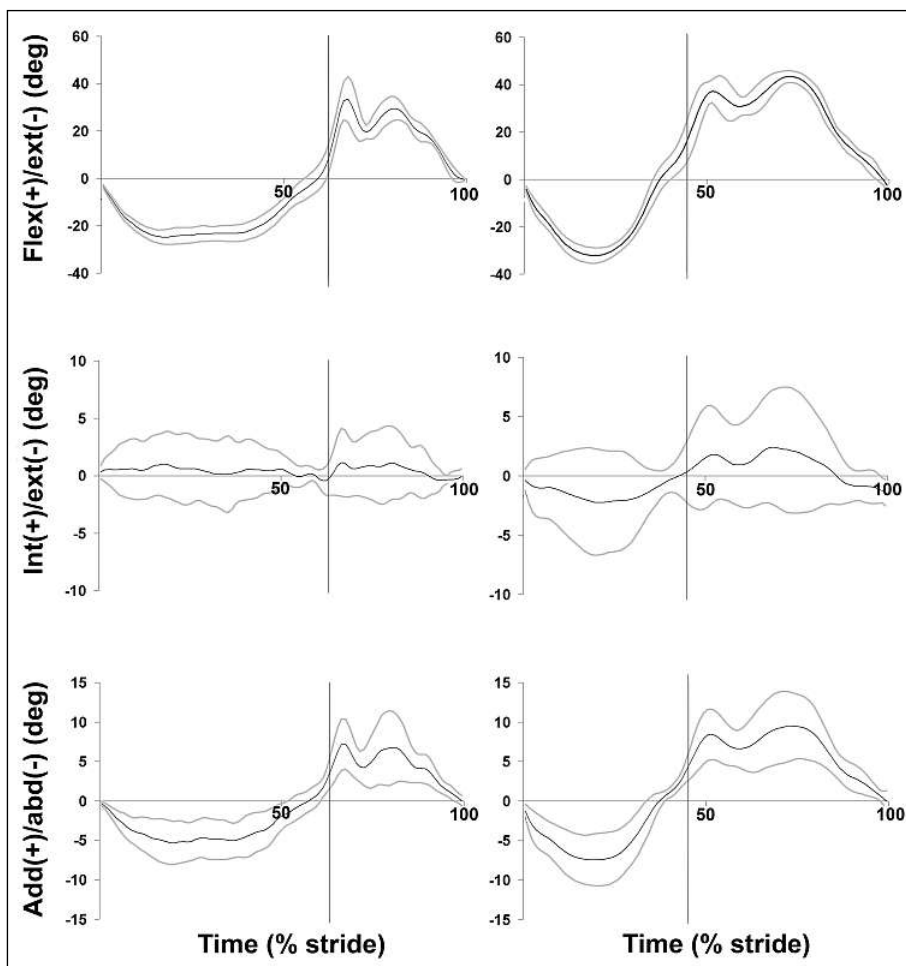


**Fig. 2** Rotational kinematics of the metacarpophalangeal joint at walk (left column) and trot (right column). Values shown are mean (black line)  $\pm$  SD (grey lines) for flexion/extension (top row), internal/external rotation (middle row) and adduction/abduction (bottom row). Vertical lines indicate the transition from stance to swing.

mental coordinate system of P1 was rotated  $+10^\circ$  (inward rotation) about its longitudinal axis, the amount of abduction during stance increased and the amount of adduction during swing increased. When the segmental coordinate system of P1 was rotated  $-10^\circ$  (outward rotation) about its longitudinal axis, the amount of abduction during stance decreased and the amount of adduction during swing decreased (Fig. 3).

Axial rotation was small in amount and variable in direction; some horses showed a little internal rotation during stance, while others showed a little external rotation. This is reflected in the fact that the standard deviation curves do not follow the shape of the mean curve. Axial rotation during swing was consistently in the opposite direction to the rotation during stance and demonstrated two peaks that corresponded temporally with the flexion peaks. Within each horse, the direction of axial rotation in the stance and swing phases was consistent for walk and trot.

## Discussion

Although the flexion/extension axis defined in the BCS in this study was not necessarily perpendicular to the sagittal plane of the horse, the shape and amplitude of the flexion/extension curves are similar to published results of sagittal plane kinematics for the walk (3) and trot (1). This is not surprising since even large misalignments of the BCS and GCS have little effect on the flexion/extension measurements where this is the predominant type of motion (5). Speed-dependent increases in stance phase extension (16) and swing phase flexion (26) have been reported previously and the results presented here suggest similar speed-dependent increases in adduction/abduction.

A variety of factors affect MCP flexion/extension including age (26), gait (27), speed (16), conformation (28) and the presence of injuries, such as capsulitis or osteoarthritis (29). Since the horses used in our study were of similar ages and sizes, it is not surprising that the flexion/extension curves showed little variability. In general, variability between horses in sagittal plane

**Table 1** Ranges of rotational motion of the metacarpophalangeal joint of the forelimb during walking ( $n=4$ ) and trotting ( $n=6$ ). Values are mean  $\pm$  SD.

|   | Range of Motion |            |            |             |            |            |
|---|-----------------|------------|------------|-------------|------------|------------|
|   | Stride          |            | Stance     |             | Swing      |            |
|   | Walk            | Trot       | Walk       | Trot        | Walk       | Trot       |
| Flexion/extension ( $^\circ$ )          | $62 \pm 7$      | $77 \pm 5$ | $31 \pm 3$ | $42 \pm 10$ | $38 \pm 7$ | $47 \pm 5$ |
| Internal/external rotation ( $^\circ$ ) | $6 \pm 3$       | $9 \pm 5$  | $4 \pm 1$  | $5 \pm 2$   | $3 \pm 2$  | $6 \pm 3$  |
| Adduction/abduction ( $^\circ$ )        | $13 \pm 7$      | $18 \pm 7$ | $7 \pm 3$  | $10 \pm 4$  | $8 \pm 4$  | $10 \pm 5$ |

kinematics has been reported to be low (30), but kinematic variability in other directions has not yet been evaluated. Results presented to date suggest greater inter-individual variability outside the sagittal plane. For example, one study reported that the MCP joint underwent lateral (external) rotation during extension (9), whereas our findings indicate differences between horses in the direction of axial rotation during stance, though individual horses were consistent between and within gaits. Individual differences in conformation of the MCP joint resulting in a medial (toed in) or lateral (toed out) deviation of the digit may be the source of inter-individual differences in axial rotation. Data from a larger number of horses will be required before conclusions can be drawn about the population as a whole and the relationships between conformation and movement patterns.

Motion outside of the sagittal plane is very sensitive to the definition of the bone coordinate systems. Kinematic crosstalk occurs when some of the flexion/extension motion appears as adduction/abduction (5). The apparent coupling of adduction/abduction with flexion/extension in our study

might have been due to kinematic crosstalk and, to investigate this possibility, the coordinate system of P1 was rotated around its longitudinal axis by  $\pm 10^\circ$ , which was considered to be the maximal error likely to be present in aligning the coordinate systems. The fact that the magnitude of adduction/abduction changed but the nature of the relationship between adduction/abduction and flexion/extension did not change, supports coupling of these two types of motion.

Other researchers have used different methods to determine the coordinate systems of the bones, which may account for differences in results. For example, Chateau et al. (8, 9) used a calibrating device to assist in orienting the local coordinate system relative to the anatomical axes of the phalanges. Problems in the assignment of bone axes are certainly not unique to animal studies. In human studies, two distinct flexion axes have been used to describe knee joint motion: the transepicondylar axis (connecting the most prominent parts of the lateral and medial condyles) and the geometric centre axis (connecting the centres of the two femoral condyles). A comparison between these methods (31) revealed sig-

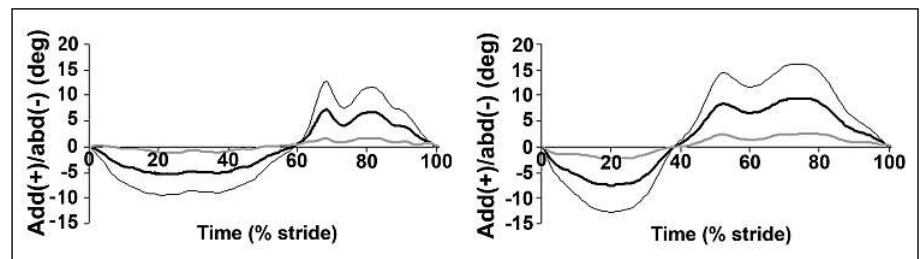


**Fig. 3** Adduction and abduction of the metacarpophalangeal joint at walk (left column) and trot (right column) for the segmental coordinate system defined in the standing pose (thick black line), after  $+10^\circ$  (inward) rotation (thin, black line) and after  $-10^\circ$  (outward) rotation (grey line) of the segmental coordinate system of the proximal phalanx around the longitudinal axis of the bone.



nificant differences in translation of the femoral condyles and tibial rotation with the geometric centre axis showing considerably more internal tibial rotation. It was concluded that, although kinematic calculations are sensitive to selection of the flexion axis, either method can be used to describe knee motion as long as the axis is clearly defined. When the data presented here are compared with those of Chateau et al. (9) for the stance phase of the trot, the curves for flexion/extension and internal/external rotation are almost identical. For adduction/abduction, there is close agreement between the curves when the P1 axis in our study was rotated outward by 10°. Thus, the differences in the results of the two studies may be a consequence of the method of assigning the segmental axes.

Joint contact forces are considerably larger during stance than during swing, so stance phase kinematics are particularly interesting in relation to the aetiology of injuries. Wild horses have pathological changes consistent with osteoarthritis in the MCP joints, with lesions on the proximo-dorsal aspect of P1 and the severity of these lesions increases with age (32). The stress of training and racing is likely to exacerbate these age-related changes. The location of lesions, such as chip fractures and osteoarthritic changes, on the dorsal margin of P1 corresponds with a dorsal shift in the contact area of the MCP joint as speed increases (17). Changes in contact area are a consequence of the increase in stance phase extension of the joint as it is more heavily loaded. Conversely, if lameness becomes established, both the amount and timing of peak MCP extension may change (33) as a consequence of reduced joint loading.

Metacarpal condylar fractures occur almost exclusively in horses which gallop at racing speed, which is associated with marked extension of the metacarpophalangeal joint during weight-bearing (34). The lateral condyle is involved in 85% of condylar fractures (35), and it will be interesting to relate these kinematic data to kinetic data which describe the joint contact forces and joint torques. Since our study has evaluated MCP kinematics only within the limited range of motion that occurs during trotting, it will be necessary to evaluate the

relationship between extension and abduction through the larger range of MCP motion that occurs at faster speeds before drawing conclusions about any possible role of MCP abduction in joint injury.

In summary, during walking and trotting, stance phase extension of the MCP joint was accompanied by abduction and swing phase flexion was accompanied by adduction. Kinetic analysis will indicate whether stance phase loading of the joint in extension and abduction is associated with large contact forces that may explain the high incidence of condylar injuries on the lateral side of the joint.

## References

- Back W, Schamhardt HC, Savelberg HHCM et al. How the horse moves: significance of graphical representations of equine forelimb kinematics. *Equine Vet J* 1995; 27: 31–38.
- Drevemo S, Johnston C, Roepstorff et al. Nerve block and intra-articular anaesthesia of the forelimb in the sound horse. *Equine Vet J* 1999; S30: 266–269.
- Hodson EF, Clayton HM, Lanovaz JL. The forelimb in walking horses: 1. Kinematics and ground reaction forces. *Equine Vet J* 2000; 32: 287–294.
- Herring L, Thompson KN, Jarret S. Defining normal three-dimensional kinematics of the lower forelimb of the horse. *J Equine Vet Sci* 1992; 12: 172–176.
- Ramakrishnan HK, Kadaba MP. On the estimation of joint kinematics during gait. *J Biomech* 1991; 24: 969–997.
- Lanovaz JL, Khumsap S, Clayton HM et al. Three-dimensional kinematics of the tarsal joint at the trot. *Equine Vet J* 2002; S34: 308–313.
- Clayton HM, Sha DH, Stick JA et al. Three dimensional kinematics of the equine carpus at trot. *Equine Vet J* 2004; 36: 671–676.
- Chateau H, Degueurce C, Denoix J-M. Evaluation of three-dimensional kinematics of the distal portion of the forelimb in horses walking in a straight line. *Am J Vet Res* 2004; 65: 447–455.
- Chateau H, Degueurce C, Denoix J-M. Three-dimensional of the distal forelimb in horses trotting on a treadmill and effects of elevation of heel and toe. *Equine Vet J* 2006; 38: 164–169.
- Clayton HM, Lanovaz JL, Schamhardt HC et al. Net joint moments and powers in the equine forelimb in the stance phase of the trot. *Equine Vet J* 1998; 30: 384–389.
- Colborne GR, Lanovaz JL, Sprigings EJ et al. Forelimb joint moments and power during the walking stance phase of horse. *Am J Vet Res* 1998; 59: 609–614.
- Lanovaz JL, Clayton HM, Colborne GR et al. Forelimb kinematics and net joint moments during the swing phase of the trot. *Equine Vet J* 1999; S30: 235–239.
- Clayton HM, Lanovaz JL, Schamhardt HC et al. Net joint moments and joint powers in equine forelimb during the stance phase of the trot. *Equine Vet J* 2000; 30: 384–389.
- Clayton HM, Schamhardt HC, Lanovaz JL et al. Net joint moments and joint powers in horses with superficial digital flexor tendinitis. *Am J Vet Res* 2000; 61: 197–201.
- Pool RR. Traumatic injury and osteoarthritis. In: Joint disease in the horse. McIlwraith CW, Trotter GW (eds). Philadelphia: W.B. Saunders Company 1996.
- McGuigan PM, Wilson AM. The effect of gait and digital flexor muscle activation on limb compliance in the forelimb of the horse *Equus caballus*. *J Exp Biol* 2003; 206: 1325–1336.
- Brama PAJ, Karssenberg D, Barneveld A et al. Contact areas and pressure distribution on the proximal articular surface of the proximal phalanx under sagittal plane loading. *Equine Vet J* 2001; 33: 26–32.
- Reinschmidt C, van den Bogert AJ, Murphy N et al. Tibiocalcaneal motion during running measured with external and bone markers. *Clin Biomech* 1997; 12: 8–16.
- Lafortune MA, Cavanagh PR., Sommer HJ et al. Three-dimensional kinematics of the human knee during walking. *J Biomech* 1992; 25: 347–357.
- van Weeren PR, van den Bogert AJ, Barneveld A. A quantitative analysis of skin displacement in the trotting horse. *Equine Vet J* 1990; S9: 101–109.
- Grood EW, Suntay WJ. A joint coordinate system for the clinical description of three-dimensional motions: applications to the knee. *J Biomech Eng* 1983; 105: 136–144.
- Soderkvist I, Wedin PA. Determining the movements of the skeleton using well-configured markers. *J Biomech* 1993; 26: 1473–1477.
- Spoor CW, Veldpaus FE. Rigid body motion calculated from spatial co-ordinates of markers. *J Biomech* 1980; 13: 391–393.
- Woltring HJ. 3-D attitude representation of human joints: a standardization proposal. *J Biomech* 1994; 27: 1399–1414.
- Mullineaux DR, Clayton HM, Gnagay LM. Effects of offset-normalizing techniques on variability in motion analysis data. *J Appl Biomech* 2004; 20: 177–184.
- Butcher MT, Ashley-Ross MA. Fetlock joint kinematics differ with age in thoroughbred racehorses. *J Biomech* 2002; 35: 563–571.
- Back W, Schamhardt HC, Barneveld A. Are kinematics of the walk related to the locomotion of a warmblood horse at the trot. *Vet Quart* 1996; 18 S2: S79–84.
- Back W, Schamhardt HC, Barneveld A. The influence of conformation on fore and hind limb kinematics of the trotting Dutch warmblood horse. *Pferdeheilkunde* 1996; 12: 647–650.
- Strand E, Martin GS, Crawford MP et al. Intra-articular pressure, elastance and range of motion in healthy and injured racehorse metacarpophalangeal joints. *Equine Vet J* 1998; 30: 520–527.

30. Degueurce C, Pourcelot P, Audigie F et al. Variability of the limb joint patterns of sound horses at trot. *Equine Vet J* 1997; S23: 89–92.
31. Most E, Axe J, Rubash H, Li G. Sensitivity of the knee joint kinematics calculation to selection of flexion axes. *J Biomech* 2004; 37: 1743–1748.
32. Cantley CE, Firth EC, Delahunt JW et al. Naturally occurring osteoarthritis in the metacarpophalangeal joints of wild horses. *Equine Vet J* 1999; 31: 73–81.
33. Keegan KG, Wilson DA, Smith BK et al. Changes in kinematic variables observed during pressure-induced forelimb lameness in adult horses trotting on a treadmill. *Am J Vet Res* 2000; 61: 612–619.
34. Parkin TD, Clegg PD, French NP et al. Risk factors for fatal lateral condylar fracture of the third metacarpus/metatarsus in UK racing. *Equine Vet J* 2005; 37: 192–199.
35. Zekas LJ, Bramlage LR, Embertson RM et al. Characterisation of the type and location of fractures of the third metacarpal/metatarsal condyles in 135 horses in central Kentucky (1986–1994). *Equine Vet J* 1999; 31: 304–308.

**Correspondence to:**

Hilary M. Clayton, DVM  
Michigan State University  
Large Animal Clinical Sciences  
D202 Veterinary Medical Center  
East Lansing, Michigan, 48824–1314 USA  
Phone: +1 517 432 5630, Fax: +1 517 432 3442  
E-mail: claytonh@cvm.msu.edu